RESEARCH ARTICLE | MAY 01 1987

Diffraction, self-focusing, and the geometrical optics limit in laser produced plasmas

R. Marchand; R. Rankin; C. E. Capjack; A. Birnboim

Phys. Fluids 30, 1521–1525 (1987)
https://doi.org/10.1063/1.866266

Diffraction, self-focusing, and the geometrical optics limit in laser produced plasmas

R. Marchand, R. Rankin, C. E. Capjack, and A. Birnboim[a)]
Department of Electrical Engineering, University of Alberta, Edmonton, Alberta, T6G 2G7 Canada

(Received 22 January 1986; accepted 27 January 1987)

The effect of diffraction on the self-modulation of an intense laser beam in an initially uniform hydrogen plasma is investigated. A formalism is used in which the diffraction term in the paraxial wave equation can be arbitrarily reduced by the use of a weight factor ι. In the limit where ι approaches zero, it is shown that the paraxial wave equation correctly reduces to the geometrical optics limit and that the problem then becomes formally equivalent to solving the ray-tracing equations. When $\iota = 1$, the paraxial wave equation takes its usual form and diffraction is fully accounted for. This formalism is applied to the simulation of self-modulation of an intense laser beam in a hydrogen plasma, for which diffraction is shown to be significant.

I. INTRODUCTION

The success of direct drive laser fusion requires that targets be irradiated with laser beams that maintain their illumination uniformity up to the critical density surface. The importance of having a uniform laser intensity is twofold. First, hot spots in modulated laser beams can stimulate resonance absorption, parametric processes, and, subsequently, the production of hot electrons. Second, if hot spots generated in the underdense plasma are able to penetrate to the critical density surface, thermal smoothing of the inward heat flux may not be sufficient to prevent fluid instabilities, such as Rayleigh–Taylor, from occurring. This latter effect may be especially important in experiments done with short wavelength lasers. For these reasons, there have been many studies made of the dynamics of intense laser beams in plasmas.[1–4] Basically, two approaches can be followed. In one, geometrical optics is assumed and the beam is modeled by a large number of rays which are governed by ray-tracing equations.[1–3] In the second approach the wave nature of the beam is retained but its direction of propagation is assumed to be mainly along a given axis. The governing equation is then the paraxial wave equation.[5–8] In both cases, refraction and inverse bremsstrahlung absorption are easily taken into account. The advantage of the geometrical optics approach is that it can readily be applied to cases where the rays are not all propagating along a given axis, or even to cases where some of the rays are reflected close to the critical density surface. On the other hand, the physical optics approach accounts for diffraction, which is important when the beam is tightly focused or modulated. In general, a comparison between the two approaches should prove useful in assessing the validity of the physical assumptions required in either case. Unfortunately, a direct comparison is not straightforward because of the very different numerical techniques used. For example, in ray-tracing codes a large number of rays must be used in order to accurately model a smoothly varying laser beam. Differences between the predictions of ray tracing and paraxial wave codes may be caused by statistical errors in accounting for the beam intensity, as well as by physical effects such as diffraction, or the beam not being paraxial.

In this article, we present a simple and convenient method for directly comparing results obtained in the geometrical optics limit with those obtained from solving the paraxial wave equation. The method consists of modifying the paraxial wave equation in such a way that diffraction can effectively be turned on or off. In the latter case the geometrical optics limit is recovered and the problem is formally equivalent to that of solving the ray-tracing equations. The general formulation of the problem is given in Sec. II and it is illustrated with a simple example in Sec. III. Results are presented in Sec. IV for the case of the modulation of an intense laser beam in an initially uniform hydrogen plasma. A summary of our results and some concluding remarks are given in Sec. V.

II. GENERAL FORMALISM

In this section, we show how the paraxial wave equation can be modified so as to artificially reduce the effect of diffraction. When diffraction is neglected, the resulting equation is shown to reduce to the proper geometrical optics limit and the problem becomes equivalent to that of solving the ray-tracing equations.

The derivation of the paraxial wave equation has been given elsewhere.[6] In short, if the laser beam propagates mainly along a given axis, say the z axis, and if the wavelength and wave period are much shorter than any other macroscopic length and time scales, respectively, the wave electric field can be expressed as

$$E(\mathbf{r},z,t) = [2\pi\omega/k(z)c^2]^{1/2}\xi(\mathbf{r},z,t) \times \exp\left(i\int_0^z dz'\, k(z') - i\omega t\right), \tag{1}$$

with $|k(z)^{-1}\,\partial\xi/\partial z|, |\omega^{-1}\,\partial\xi/\partial t| \ll |\xi|$. In Eq. (1) $\mathbf{r}$ is the position vector in the plane perpendicular to z and the local wave vector $k(z)$ is defined by the local dispersion relation $\omega^2 = k^2(z)c^2 - \omega_p^2(z)$, ω_p being the plasma frequency as a function of z, evaluated at a conveniently chosen radius, say r_0, which may also be a function of z. In the following, for simplicity, we assume that $\mathbf{r}_0 = \mathbf{0}$. Substituting Eq. (1) into

[a)] Present address: ADA, P.O. Box 2250 (24), Haifa 31021, Israel.

 0031-9171/87/051521-05$01.90

Maxwell's equations yields the paraxial wave equation

$$\frac{\partial \xi}{\partial z}+\frac{1}{v_g(z)}\frac{\partial \xi}{\partial t}=\frac{i}{2k(z)}\nabla_\perp^2\xi-\frac{i}{2k(z)}Q\xi\,, \tag{2}$$

where $v_g(z)=k(z)\,c^2/\omega$ is the beam group velocity, $\nabla_\perp^2$ is the Laplacian in the coordinates perpendicular to the z axis, and

$$Q=\frac{\omega_p^2(\mathbf{r},z)}{c^2}\left(1-\frac{n(o,z)}{n(\mathbf{r},z)}\right)-ik(z)K_{\rm abs}(r,z) \tag{3}$$

accounts for refraction (real part) and inverse bremsstrahlung attenuation[9] (imaginary part). In Eq. (3), $\omega_p(\mathbf{r},z)$ and $n(\mathbf{r},z)$ are the plasma frequency and free electron density as a function of $\mathbf{r}$ and z, respectively.

The method used to study the effect of diffraction is essentially the same as the one used elsewhere to model spatial beam incoherency in a well underdense plasma.[10] It consists of multiplying and dividing, respectively, the diffractive ($\nabla_\perp^2$) and refractive (Q_r) terms in Eq. (2) by a constant ι which can be varied between 0 and 1. It was shown in Ref. 9 that for plasma densities much less than critical, i.e., $k(z)\simeq k_0$, this prescription preserves the correct ray-tracing equations in the limit where geometrical optics is valid. We now extend the proof to cases where the z dependence of the local wave vector is non-negligible, and show that in the limit where ι approaches zero, Eq. (2) formally reduces to the geometrical optics limit. This is done by considering the Wigner integral[11]

$$f(\mathbf{r},z,t,\mathbf{k})=\int\frac{d^2r'}{2\pi}\,\xi^*\left(\mathbf{r}+\frac{\mathbf{r}'}{2},z,t\right)\xi\left(\mathbf{r}-\frac{\mathbf{r}'}{2},z,t\right)\times\exp(ik_\perp\cdot\mathbf{r}')\,. \tag{4}$$

An equation for f can be obtained from Eqs. (2) and (3). We find, after modifying the diffractive and refractive terms as prescribed above,

$$\begin{aligned}&\frac{\partial f}{\partial z}+\frac{1}{v_g(z)}\frac{\partial f}{\partial t}+\frac{\iota\mathbf{k}_\perp}{k(z)}\cdot\nabla_\perp f-\frac{\nabla_\perp Q_r}{2\iota k(z)}\cdot\frac{\partial f}{\partial\,\mathbf{k}_\perp}+\frac{Q_i}{k(z)}f\\&=\frac{i}{2k(z)}\int\frac{d^2r'}{2\pi}\left[\hat{Q}^*\left(\mathbf{r}+\frac{\mathbf{r}'}{2}\right)-\hat{Q}^*(\mathbf{r})-\frac{\mathbf{r}'}{2}\cdot\nabla_\perp\hat{Q}^*(\mathbf{r})-\hat{Q}\left(\mathbf{r}-\frac{\mathbf{r}'}{2}\right)+\hat{Q}(\mathbf{r})-\frac{\mathbf{r}'}{2}\cdot\nabla_\perp\hat{Q}(\mathbf{r})\right]\xi^*\left(\mathbf{r}+\frac{\mathbf{r}'}{2},z,t\right)\xi\left(\mathbf{r}-\frac{\mathbf{r}'}{2},z,t\right)\\&\times\exp(i\mathbf{k}_\perp\cdot\mathbf{r}')\,,\end{aligned} \tag{5}$$

where $\hat{Q}=Q_r/\iota+iQ_i$. With the change of variables $\kappa=\iota\mathbf{k}_\perp$, and $\boldsymbol{\rho}=\mathbf{r}'/\iota$, this equation becomes

$$\begin{aligned}&\frac{\partial f}{\partial z}+\frac{1}{v_g(z)}\frac{\partial f}{\partial t}+\frac{\boldsymbol{\kappa}}{k(z)}\cdot\nabla_\perp f-\frac{\nabla_\perp Q_r}{2k(z)}\cdot\frac{\partial f}{\partial\kappa}+\frac{Q_i}{k(z)}f\\&=\frac{i\iota^2}{2k(z)}\int\frac{d^2\rho}{2\pi}\left[\hat{Q}^*\left(\mathbf{r}+\iota\frac{\rho}{2}\right)-\hat{Q}^*(\mathbf{r})-\iota\frac{\rho}{2}\cdot\nabla_\perp\hat{Q}^*(\mathbf{r})-\hat{Q}\left(\mathbf{r}-\iota\frac{\rho}{2}\right)+\hat{Q}(\mathbf{r})-\iota\frac{\boldsymbol{\rho}}{2}\cdot\nabla_\perp\hat{Q}(\mathbf{r})\right]\xi^*\left(\mathbf{r}+\iota\frac{\boldsymbol{\rho}}{2},z,t\right)\xi\left(\mathbf{r}-\iota\frac{\boldsymbol{\rho}}{2},z,t\right)\\&\times\exp(i\mathbf{k}\cdot\boldsymbol{\rho})\,.\end{aligned} \tag{6}$$

It is clear that for any reasonably well-behaved function Q, the right side of Eq. (6) vanishes in the limit where ι approaches zero. Hence, in that limit the paraxial wave equation is equivalent to a first order partial differential equation for the distribution function f, with characteristics given by

$$\frac{d\mathbf{r}}{dz}=\frac{\boldsymbol{\kappa}}{k(z)}\,, \tag{7}$$

$$\frac{d\boldsymbol{\kappa}}{dz}=\frac{-\nabla_\perp Q_r}{2k(z)}\,, \tag{8}$$

or equivalently,

$$\frac{d}{dz}\left(\mu(o,z)\frac{d\mathbf{r}}{dz}\right)=\nabla_\perp\mu(\mathbf{r},z)\,, \tag{9}$$

where use has been made of the relation between $k(z)$, Q_r, and the index of refraction μ; $k(z)=\mu(0,z)k_0$ and $Q_r=k_0^2[\mu^2(0,z)-\mu^2(\mathbf{r},z)]$, where $k_0=\omega/c$ is the wave vector of the beam in vacuum. For comparison, the equation governing rays in the geometrical optics limit is given by[12]

$$\frac{d}{ds}\left(\mu\frac{d\mathbf{x}}{ds}\right)=\nabla\mu\,, \tag{10}$$

where μ is the index of refraction as a function of $\mathbf{r}$ and z, $\mathbf{x}=\mathbf{r}+z\hat{z}$ is the three-dimensional position vector, and ds is the element of length measured along the ray trajectory.

We now show that Eq. (10) reduces to Eq. (9) in the paraxial limit when μ is maximum on axis, or when the plasma density is well below critical. In the paraxial limit, d/ds can be approximated by d/dz in Eq. (10). Also, assuming that μ is parabolic in r with a maximum on axis, i.e., $\mu(\mathbf{r},z)\simeq\mu(0,z)(1-\alpha{:}\mathbf{rr})$, where α is a positive definite 2×2 matrix, the largest angle between the ray trajectory and the z axis can be estimated to be of order $a\sqrt{\lambda}$, where a is the maximal radial excursion and λ is the largest eigenvalue of α. Thus, in the paraxial limit, because $a\sqrt{\lambda}\ll1$, μ can be approximated to lowest order by $\mu(0,z)$ in the left side of Eq. (10). Of course, the $\mathbf{r}$ dependence of μ in the right side of Eq. (10) cannot be neglected because it contributes to the perpendicular component of the gradient to lowest nonvanishing order. Hence, the perpendicular component of Eq. (10) reduces approximately to Eq. (9). It is worth noting that the assumption concerning the parabolic dependence of μ, with a maximum on axis, is not needed if the plasma is well underdense. In that case, $\mu\simeq1$ to lowest order in the left-hand side, and the perpendicular component in Eq. (10) again reduces to Eq. (9).

III. EXAMPLE PROBLEM

In this section we illustrate the technique just described with a simple example: that of a Gaussian beam propagating in a parabolic waveguide. To be specific, the electron density is assumed to be axially uniform and to vary in r according to

$$n_e(r)=n_0(1+r^2/a^2)\,. \tag{11}$$

Attenuation caused by inverse bremsstrahlung is neglected for simplicity. It is well known that the standard (with $\iota=1$) paraxial wave equation admits solutions corresponding to the intensity

$$I(r,z)=[I_0/\pi\sigma(z)^2]\exp[-r^2/\sigma(z)^2]\,, \tag{12}$$

where $\sigma(z)$ is a periodic function of z.[13] The solution of our model paraxial wave equation (with the diffractive and the refractive terms, respectively, multiplied and divided by ι) is very similar to that of the standard case. It can be shown that it also admits solutions corresponding to the intensity given in Eq. (12), with

$$\sigma(z) = \sigma_0\{\cos^2(Kz) + [\sin^2(Kz)]/(kK\sigma_0^2/\iota)^2\}^{1/2}, \tag{13}$$

where $\sigma_0 = \sigma(z=0)$, $k = (\omega/c)[1-\omega_p^2(0)/\omega^2]^{1/2}$, and $K = \omega_p(0)/kca$, $\omega_p(0)$ being the plasma frequency computed at $r=0$. In the derivation of Eq. (13) it is assumed, without loss of generality, that σ has an extremum at $z=0$. It is easy to verify that Eq. (13) agrees with the predictions of geometrical optics in the limits where $\iota \to 0$,[14] and with those of standard physical optics when $\iota = 1$.[15]

An interesting point to note about Eq. (13) is that, if $\sigma_0 = (\iota/kK)^{1/2}$, then $\sigma(z) = \sigma_0$ is independent of z. This value of σ is the radius of the so-called lowest radial eigenmode. Also, if $\sigma_{\min}$ and $\sigma_{\max}$ represent the minimum and maximum values of σ, it can be seen that $\sigma_{\min}\sigma_{\max} = \iota/kK$; i.e., the radius of the lowest order eigenmode is the geometric mean of minimum and maximum radii. An important property of Eq. (13) is that the period of oscillation π/K is independent of ι. This is because, as explained in the previous section, the paraxial wave equation has been modified in such a way as to preserve the proper ray-tracing equations. Finally, the radius of the lowest eigenmode is seen to approach zero, as ι approaches zero. Equivalently, for a given σ_o, the beam can be made to focus into an arbitrarily small spot at $z = \pi/2K$, by taking ι sufficiently small. This is why ι can be thought of as a knob with which diffraction can be reduced by an arbitrary amount.

We now turn to the numerical implementation of this simple example. Specifically, we consider a 0.266 μm laser beam propagating in a waveguide with an electron density on axis equal to 10% of the critical density, and a radial density scale length $a = 252$ μm. The period of oscillation and the lowest mode radius (with $\iota = 1.0$) are then $\pi/K = 2.5$ mm and $(kK)^{-1/2} = 5.96$ μm, respectively. The paraxial wave equation is solved numerically using cubic splines on a uniform 40×40 grid extending 18 μm in r and 5 mm in z. The radius of the incident beam is always set equal to the $\iota = 1$ lowest eigenmode radius, $\sigma_0 = 5.96$ μm.

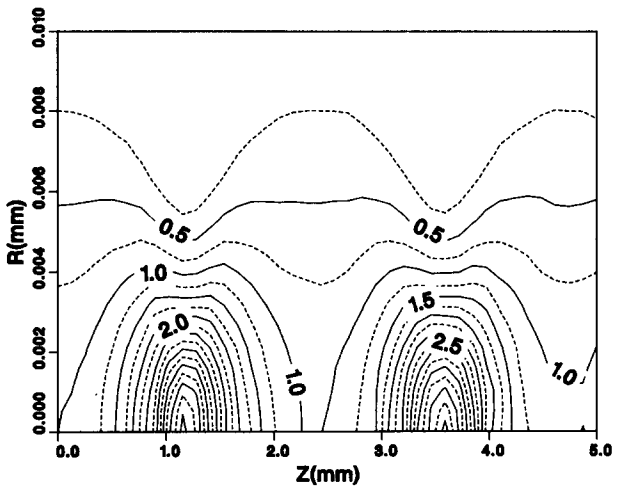

FIG. 1. Contour lines of the laser flux computed for the $\iota = 0.5$ test case of Sec. III. The flux is normalized with respect to the maximum incident value.

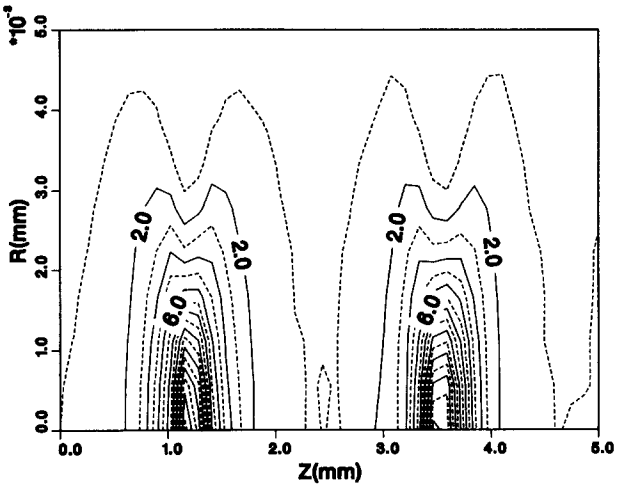

FIG. 2. Same as Fig. 1, except that $\iota = 0.25$.

Results are shown in Figs. 1 and 2 for $\iota = 0.5$ and $\iota = 0.25$, respectively, for which Eq. (13) predicts radii $\sigma/\sigma_0 = 0.5$ and 0.25 at the foci. The intensity on axis should then be, respectively, 4 and 16 times that at $z=0$. The contour plots show intensities slightly in excess of these values. This is because errors introduced by the use of a finite grid in the solution of the wave equation. In particular, the lowest order mode radius is found numerically to be smaller than the analytic value by approximately 5%. The important features to note about Figs. 1 and 2, however, are that the spot size at the focus does scale as predicted analytically, and the focusing length is independent of ι.

IV. SELF-FOCUSING

We now use the formalism described in Sec. II to assess the effect of diffraction during the self-modulation of an intense laser beam in a hydrogen plasma. Specifically, we consider one of the cases presented in Ref. 3. A 266 nm Gaussian laser beam is incident on an initially uniform fully ionized hydrogen plasma with $T_e = 1$ keV, $T_e/T_i = 30$, and an electron density $n_e = 2.52\times10^{21}$ cm^{-3}. For the above wavelength, n_e is 0.16 of the critical density. Initially, the incident laser intensity on axis is assumed to rise instantaneously from zero to $I_0 = 10^{15}$ W/cm^2. This input intensity remains constant thereafter. The radial profile of the incident beam is Gaussian; i.e., $I(r,z=0) = I_0\exp(-r^2/\sigma^2)$, with $\sigma = 300$ μm, corresponding to a FWHM of 0.5 mm. In the simulation, the plasma and laser beam are assumed to be cylindrically symmetric. A two-dimensional Eulerian code is used to model the plasma dynamics on a 40×40 mesh of dimension 1 and 5 mm in the r and z directions, respectively. The electron heat conductivity is taken as the harmonic mean of the Spitzer and the free-streaming values, with a flux limiter of 3%. The paraxial wave equation is solved in cylindrical geometry using cubic splines.[6] The laser–plasma interaction includes inverse bremsstrahlung absorption and refraction. The importance of diffraction is estimated by comparing re-

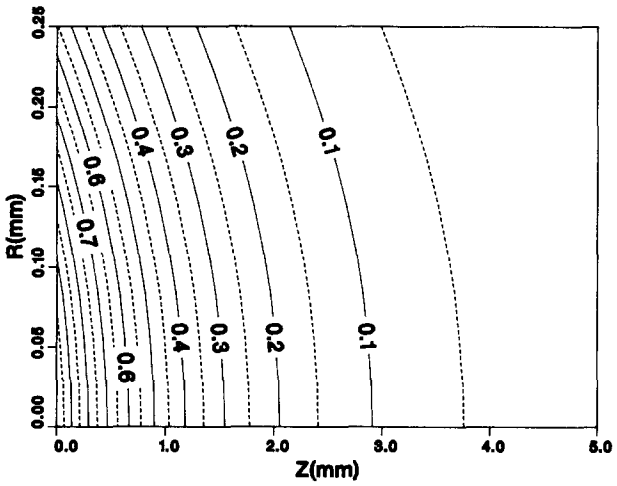

FIG. 3. Contour lines of the laser flux at time $t = 0$. The flux is normalized with respect to its maximum incident value. The laser beam is incident from the left.

sults obtained with $\iota = 1.0$ and $\iota = 0.5$. Although the paraxial wave solver used in the simulations can account for the ponderomotive force, this force is ignored for consistency with Ref. 3.

Figure 3 shows the contour lines of the laser flux at the beginning of the simulation. Initially, the laser beam is well collimated. As it propagates into the plasma, it is attenuated by inverse bremsstrahlung absorption without any refraction, or significant diffraction.

Figure 4 shows the electron density and the laser flux computed at 1 nsec with diffraction fully taken into account ($\iota = 1$). For comparison, Fig. 5 shows those profiles computed at the same time, but when diffraction is artificially reduced by selecting $\iota = 0.5$. The density profiles in Figs. 4(a) and 5(a) are qualitatively similar and show a number of interesting features. As expected, the plasma is heated near the axis, and made to expand outwards. There results a minimum in the electron density near the axis, which is responsible for focusing the laser beam. There is also a steep density gradient along $r = 0.5$, $z = 1.0$ mm and $r = 0.2$, $z = 2.5$ mm. This front is caused by the sudden heating of the plasma near the axis, and it propagates outward at approximately the sound speed. In Figs. 4(b) and 5(b) the laser beam self-focuses off axis at approximately $z = 2$ mm. Foci also occur near $z = 4$ mm. In Fig. 4(b), the 4 mm focus lies on axis, while in Fig. 5(b), it is positioned near the axis. The simulation done with reduced diffraction ($\iota = 0.5$), however, yields a maximum intensity at the first focus that is a

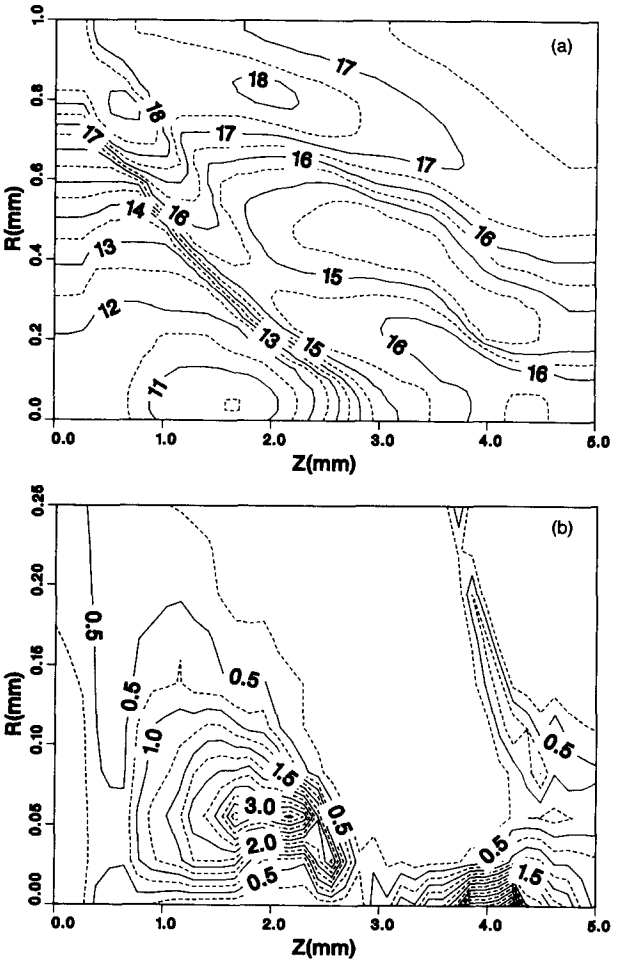

FIG. 4. Contour lines of electron density (a) and the laser flux (b) computed with diffraction ($\iota = 1.0$) at 1 nsec. The electron density is in percent of the critical density. The laser flux is normalized with respect to its maximum incident value.

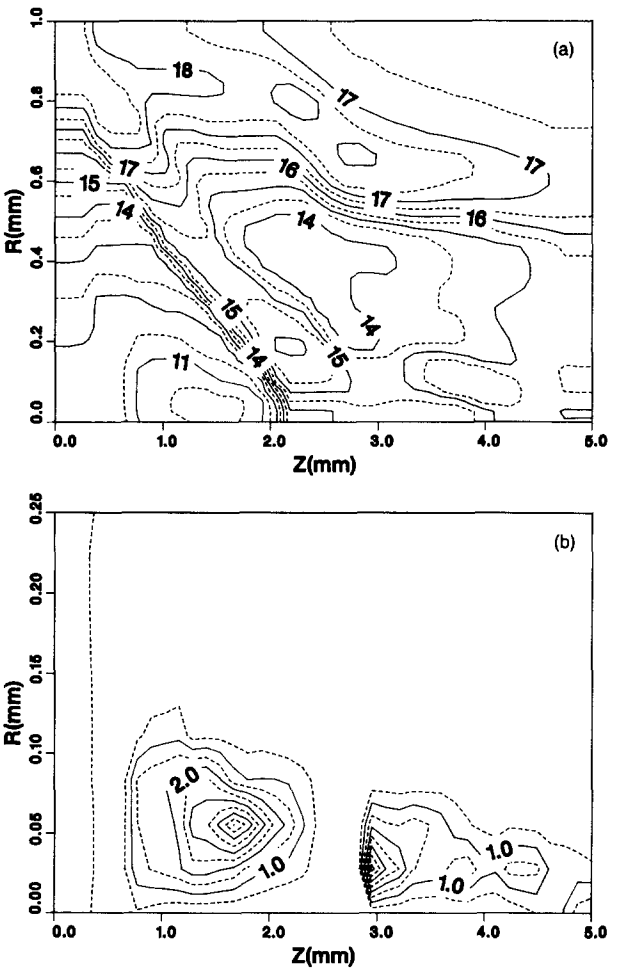

FIG. 5. Same as in Fig. 4, but computed when diffraction is turned down ($\iota = 0.5$).

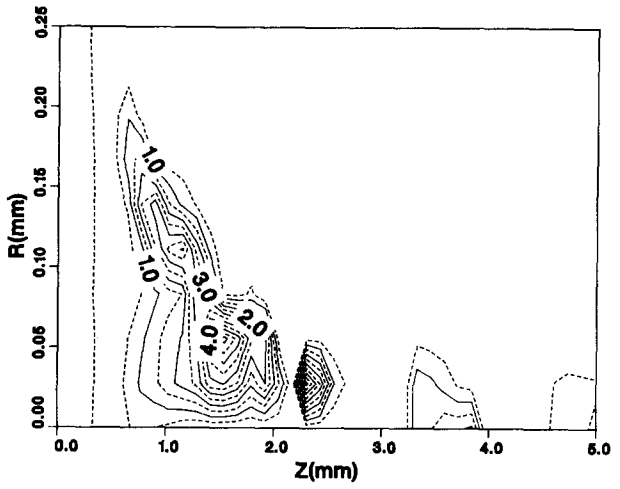

FIG. 6. Contour lines of the laser flux computed with reduced diffraction ($\iota = 0.5$), but using the same plasma density and temperature profiles as those that resulted in Fig. 4. The laser flux is normalized with respect to its maximum incident intensity.

factor 1.4 larger than that computed with $\iota = 1$. Correspondingly, the variation in the laser intensity takes place on a shorter scale length when diffraction is reduced. The situation is different with the on-axis focus, where the laser intensity is higher when computed with $\iota = 1$. We note, incidentally, that the position of the on-axis foci observed here is in reasonable agreement with the 5 mm focusing length read from Fig. 4(b) of Ref. 3.

The results shown in Figs. 4 and 5 are obtained by advancing the fluid and laser wave equations for many time steps and it may be thought possible that the differences observed arise because of the accumulation of a large number of small errors. Thus, in order to single out the effects of diffraction, we show, in Fig. 6, the laser flux computed with $\iota = 0.5$, but using the same plasma density and temperature profiles as those which resulted in Fig. 4. The only source of differences between Figs. 4(b) and 6 is the reduction of diffraction in Fig. 6. These differences are seen to be considerable, and are qualitatively similar to those that occur in Figs. 4(b) and 5(b). In particular, the intensity is larger at the first focus, and modulations occur on a shorter scale length when diffraction is reduced.

V. SUMMARY AND CONCLUSION

We present a simple method for estimating the importance of diffraction using the paraxial wave equation and a variable weighting parameter ι. The importance of diffraction is assessed directly, by comparing results obtained with different values of ι. The method consists of multiplying and dividing the diffractive term (the Laplacian) and the refrac tive term (the real part of Q) in the wave equation, respec tively, by an arbitrary constant ι. When $\iota = 1$, the paraxia wave equation has its usual form and diffraction is correctl taken into account. In the limit where ι approaches zero however, diffraction becomes negligible and the wave equa tion formally reduces to the geometrical optics limit ir which the usual ray-tracing equations are recovered.

The formalism is used to assess the effects of diffractio on the self-focusing of an intense laser beam in an initiall spatially uniform fully ionized hydrogen plasma. The cas examined has also been considered in Ref. 3 where diffrac tion was not accounted for. Diffraction is found here to pla a significant role in the propagation of the beam since, i effect, it reduces the laser intensity at the foci of the fila ments, and thus causes the beam modulations to becom spatially smoother. We recall that the ponderomotive forc has not been included in our simulations. Because the effec of the ponderomotive force is expected to be particularl important in regions where the laser intensity varies on short scale length, it follows that diffraction should also b important when modeling laser beam filamentation, whic is driven primarily by the ponderomotive force.

ACKNOWLEDGMENTS

We would like to thank Dr. K. Estabrook for some use ful conversations. We also wish to thank the referees fo making several constructive comments.

This work was supported by the Natural Sciences an Engineering Research Council of Canada.

[1] S. Sartang, R. Evans, and W. T. Toner, J. Phys. D **16**, 955 (1983).
[2] R. S. Craxton and R. L. McCrory, J. Appl. Phys. **56**, 108 (1984).
[3] K. Estabrook, W. L. Kruer, and D. S. Bailey, Phys. Fluids **28**, 19 (1985)
[4] C. E. Max, in *Laser Plasma Interaction*, edited by R. Balian and J. C Adam (North-Holland, Amsterdam, 1982), pp. 301–410, and reference therein.
[5] J. A. Fleck, Jr., J. Comput. Phys. **16**, 324 (1974).
[6] J. N. McMullin, C. E. Capjack, and C. R. James, Comput. Phys. Comm **23**, 31 (1981).
[7] J. A. Stamper, R. H. Lehmberg, A. Schmitt, M. S. Herbst, F. C. Young, J H. Gardner, and S. P. Obenschain, Phys. Fluids **28**, 2563 (1985).
[8] J. D. Nicholas and S. G. Sajjdi, J. Phys. D **19**, 737 (1986).
[9] T. W. Johnston and J. Dawson, Phys. Fluids **16**, 722 (1973).
[10] R. Marchand, C. E. Capjack, and C. R. James, J. Appl. Phys. **57**, 732 (1985).
[11] F. Tappert, J. Opt. Soc. Am. **66**, 1368 (1976).
[12] M. Born and E. Wolf, *Principles of Optics* (Pergamon, Oxford, 1975), 5th ed., p. 122.
[13] H. Kogelnik, Appl. Opt. **4**, 1562 (1965).
[14] J. T. Verdeyen, *Laser Electronics* (Prentice–Hall, Englewood Cliffs, NJ 1981).
[15] J. N. McMullin, C. E. Capjack, and C. R. James, Phys. Fluids **21**, 1828 (1978).